Scripta Materialia 144 (2018) 78–83

Contents lists available at ScienceDirect

Scripta Materialia

journal homepage: www.elsevier.com/locate/scriptamat

Regular article

Dynamic interaction between grain boundary and stacking fault tetrahedron

Liang Zhang [a,b,*], Cheng Lu [a,*], Kiet Tieu [a], Yasushi Shibuta [b]

[a] School of Mechanical, Materials and Mechatronic Engineering, University of Wollongong, Wollongong, NSW 2522, Australia
[b] Department of Materials Engineering, University of Tokyo, Bunkyo-ku, Tokyo 113-8656, Japan

ARTICLE INFO

Article history:
Received 27 July 2017
Received in revised form 31 August 2017
Accepted 17 September 2017
Available online xxxx

Keywords:
Molecular dynamics
Grain boundary
Vacancy
Dislocation

ABSTRACT

We utilize molecular dynamics simulations to investigate the dynamic interaction between the grain boundary (GB) and the stacking fault tetrahedron (SFT) in bicrystal copper. The grain boundary can migrate itself under the shear strain and can serve as a sink to remove SFT. The sink efficiency of grain boundaries is sensitive to their structural characteristics. The high-angle GBs can show a great ability to remove SFT even at an extreme low temperature, while the increase of temperature can facilitate the annihilation of SFT at the low-angle GBs. This study reveals a new possible GB-mediated damage healing mechanism of irradiated materials.

High-energy particles, such as neutron, proton, and ions, will develop point defects or defect clusters in materials under irradiation environment [1–3]. These defects may subsequently evolve into microstructural flaws which could deteriorate the physical properties of the irradiated materials and led to the direct structural failure [4,5]. Stacking fault tetrahedron (SFT) is a dominant type of vacancy cluster in various of irradiated face-centered cubic (fcc) metals due to its favorable structure that contains close-packed planes [6–9]. The structure of SFT is highly stable so that can act as a strong obstacle to the gliding dislocations, which results in hardening, embrittlement and plastic instabilities of materials [10,11]. The efficient removal of high-density SFTs is necessary to minimize void swelling and alleviate radiation hardening. However, the removal of SFT is very challenging and typically requires annealing at very high temperatures [12], incorporation of interstitials [13], or interaction with mobile dislocations [14].

It was reported that nanocrystalline materials had shown an improved radiation resistance compared to their coarser grained counterparts [15–18]. There are recently increasing interests on radiation tolerance of nanostructured materials because they possess a significant fraction of interfaces or grain boundaries (GBs) which can lead to the reduction of irradiation-induced defects [19–24]. The assumption that grain boundary can absorb point defects was confirmed by previous experimental observations. For examples, Chimi et al. [25] studied the effects of ion irradiation on nanocrystalline Au and showed that the irradiation-produced defects were thermally unstable because of the existence of a large volume fraction of GBs. Nita et al. [11] investigated the irradiation impact on the microstructure in nanostructured Ni and Cu specimens that were synthesized by electrodeposition and severe plastic deformation. They found that the irradiation-induced microstructure consists exclusively of SFTs, and the GB could be a major sink for the defects which resulted in a much lower density of SFTs than in the case of coarser grained material. The experimental findings suggest a possibility of the design and fabrication of radiation tolerant materials by reducing the grain size or via GB engineering. Meanwhile, the understanding of how defects interact with GB at the atomic scale is still in progressing [24,26–28]. In particular, while GB can provide a large energetic driving force for self-interstitial atoms (SIAs) to aggregate on the GB, the radiation-induced vacancies and their clusters (e.g., voids and SFTs) usually show a less mobility than the SIAs [10,13,22,29]. In some irradiation experiments, the vacancy defects became nearly immobile under a low-temperature condition [25,30,31]. Nevertheless, the annihilation of vacancies was still somehow enhanced by grain boundaries in these experiments, indicating the alternative GB-mediated mechanisms instead of the conventional vacancy diffusion mechanism that can assist the annihilation of vacancy defects within grain interiors. Atomistic simulations offered an opportunity to study the GB behaviors since the deformation conditions can be controlled and a detailed investigation of the underlying atomic scale processes can be made [32]. For example, by using molecular dynamics (MD) simulations, Bai et al. [13] proposed a 'recombination mechanism' at GB, i.e., the radiation-induced interstitials were firstly absorbed by the GB to form an interstitial-rich GB which can promote the vacancy-interstitial recombination subsequently. In this study, MD simulations were carried out to investigate the interaction between the shear-

* Corresponding authors at: School of Mechanical, Materials and Mechatronic Engineering, University of Wollongong, Wollongong, NSW 2522, Australia.
E-mail addresses: lz592@uowmail.edu.au (L. Zhang), chenglu@uow.edu.au (C. Lu).

https://doi.org/10.1016/j.scriptamat.2017.09.027
1359-6462/

coupled GB motion and SFT in bicrystal Cu. We found that the migrating GB can serve as a sink to remove SFT intragrain. Also, it was found that GB structure and temperature can have a significant influence on the sink efficiency.

The simulations were conducted using the parallel molecular dynamics code LAMMPS [33] with the embedded-atom method (EAM) potential for Cu [34]. The dimensions of each constructed bicrystal model were approximately 108 Å × 146 Å × 108 Å (X × Y × Z), and the total number of atoms was about 1.5×10^5. The GB was obtained by rotating grain-A and grain-B along [001] tilt axis, and the SFT was placed in grain-A, as shown in Fig. 1(a). Four symmetric tilt GBs were taken into consideration in this study; they are Σ5(310) ($\theta = 36.9°$) GB, Σ5(210) ($\theta = 53.1°$) GB, Σ37(750) ($\theta = 71.1°$) GB, and Σ61(650) ($\theta = 79.6°$) GB. The four GBs were intentionally selected to represent both of the high-angle GB and the low-angle GB. Due to the symmetry of the fcc lattice, the misorientation angles from 0° to 90° covered all the distinct boundary structures of <100> tilt GBs so that any GB that with the misorientation angle close to 0° or 90° was referred to the low-angle GB. Here, we tentatively defined the Σ37 GB and Σ61 GB as the low-angle GBs, while the two Σ5 GBs were regarded as the high-angle ones. The detailed GB structures are shown in Fig. 1(b) where all the GBs contain topologically identical structural units, as outlined by the red line. They differ only by the distance separating the structural units and by their positions relative to the GB plane, consisting either a flat (Σ5, Σ61) or a zigzag (Σ37) boundary plane. In particular, the structure of the two low-angle GBs can be described as an array of discrete perfect dislocations ($\mathbf{b} = 1/2[\bar{1}10]$), and the dislocation cores are formed by the structural units. The SFT was generated by introducing an equilateral triangular plate of vacancies in the (111) plane in grain-A. The triangular platelet contained 55 vacancies, 10 on each edge. After the energy minimization procedure, the vacancy plate evolved to an SFT followed the Silcox-Hirsch mechanism [35]. The size of the SFT is about 2.3 nm long on each edge, which is similar to the size of SFTs in copper observed in the experiment [36].

To simulate the coupled GB motion, we followed the previous method [37] to apply a shear deformation to the bicrystal model. The shear velocity was set as $V_s = 2$ m/s throughout the simulation, and the time increment of simulations was fixed at 2 fs. By considering the effect of temperature, the simulations were carried out at 10 K, 300 K and 600 K respectively. Simulation results show that the GBs can show a normal motion (V_n) under shear in all studied cases. Specifically, when the stress reached a critical level, the GB jumped upwards abruptly from its original place to another equilibrium position, accompanied by the release of local stress concentration [38]. The GB kept stationary until the energy barrier was overcome to reach the next local energy minimum as the shear strain progressed. This periodic process keeps driving the motion of the boundary and results in the GB migration upwards, as shown in the *supplementary videos*.

The migrating GB swept up the SFT in grain-A as it passed by, and some different interactions have been observed depending on the GB characteristics. Fig. 2 shows the snapshots of interactions between GBs and the preexisting SFT at 10 K. For Σ5(310) GB, the boundary plane moved upwards under shear and reached the SFT at about 0.7 ns. The SFT annihilated gradually into the boundary plane as the GB migration progressed, and it was eventually absorbed by the GB, leaving behind a defect-free area, as shown in Fig. 2(a). The same scenario was observed for Σ5(210) GB, where the SFT was completely removed by the migrating boundary plane, as shown in Fig. 2(b). In the case of Σ37(750) GB, the SFT was destructed by the migrating GB at 10 K, but the absorption of the SFT was incomplete. While the major part of the SFT structure was removed, the rest part broken down into the mono-vacancies and the small vacancy cluster, as shown in Fig. 2(c). By checking the enlarged image, the total number of the remanent vacancies was counted as $n = 7$. For Σ61(650) GB, the tetrahedral structure was retained after the GB passed through the SFT, although the arrangement of atoms at the edges of the SFT became less regular, as shown in Fig. 2(d). The simulation results obtained at the extreme low temperature indicate that the GB structure can play a significant role in the removal of SFT. The high-angle GBs show a strong ability to annihilate the SFT, while the sink efficiency for absorbing SFT of the low-angle GBs is relatively weak or even not evidenced. This finding qualitatively agrees with the experimental results where the increased radiation tolerance was reported in the nanostructured materials which possess a large proportion of high-angle GBs [3]. On the other hand, the temperature in some irradiation experiments are so low (for instance, 100 K [25]) that the conventional vacancy diffusion mechanism is less possible functioned. The simulations conducted at 10 K in this study, in particular for the high-angle GBs, revealed a possible GB-mediated mechanism that can assist the removal of vacancy defects at low temperature.

It is known that the structure of SFT consists of six stair-rod dislocations along the edges of the tetrahedron and the staking fault on the four {111} planes [7]. On the other hand, the low-angle GB can be regarded as composed of an array of discrete dislocations. Therefore, the interaction between the low-angle GB and the SFT can be interpreted as a serial of dislocation activities. To further understand the low-angle GB-SFT interaction, the dislocation extraction algorithm [39,40] was used to

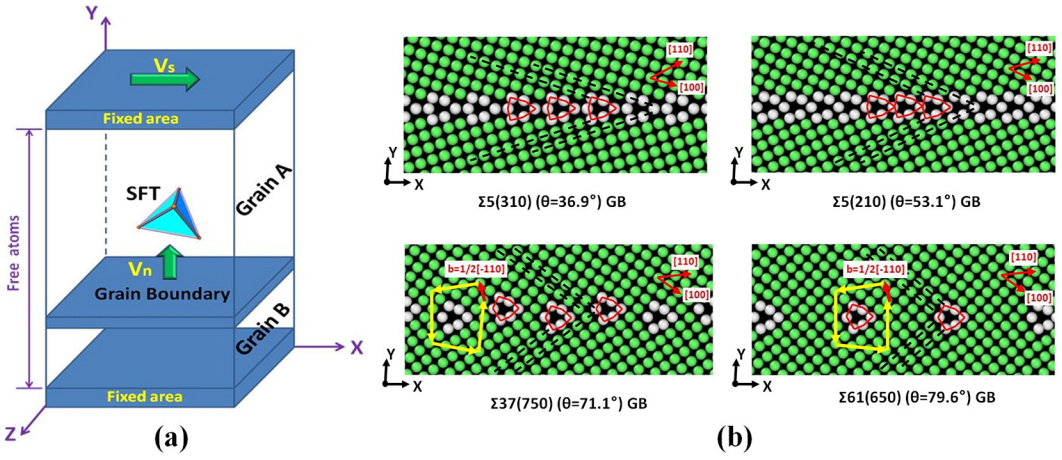

Fig. 1. (a) Schematic of the simulation model. (b) Atomic images of the equilibrium structure of Σ5(310) ($\theta = 36.9°$) GB, Σ5(210) ($\theta = 53.1°$) GB, Σ37(750) ($\theta = 71.1°$) GB, and Σ61(650) ($\theta = 79.6°$) GB. The GB structures are viewed along the [001] tilt axis and are colored according to the common neighbor analysis (CNA) parameter. The structural units are outlined by the red line. The Burgers vectors of the dislocations were determined by the standard Burgers circuit, as indicated by the yellow and red arrows. (For interpretation of the references to color in this figure legend, the reader is referred to the web version of this article.)